



Activation of TMEM16A Ca^{2+} -activated Cl^- channels by ROCK1/moesin promotes breast cancer metastasis



Shuya Luo^a, Hui Wang^a, Lichuan Bai^a, Yiwen Chen^a, Si Chen^b, Kuan Gao^a, Huijie Wang^a, Shuwei Wu^a, Hanbin Song^a, Ke Ma^a, Mei Liu^a, Fan Yao^c, Yue Fang^b, Qinghuan Xiao^{a,*}

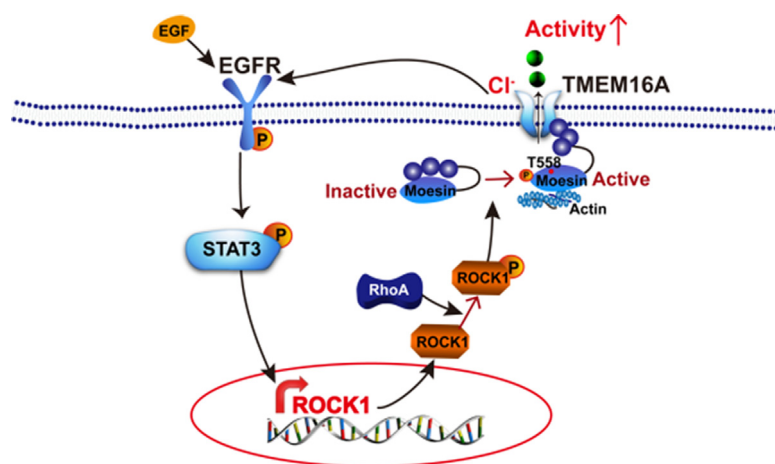
^a Department of Ion Channel Pharmacology, School of Pharmacy, China Medical University, Shenyang 110122, China

^b Department of Microbial and Biochemical Pharmacy, School of Pharmacy, China Medical University, Shenyang 110122, China

^c Department of Breast Surgery and Surgical Oncology, Research Unit of General Surgery, The First Affiliated Hospital of China Medical University, Shenyang 110001, China

GRAPHICAL ABSTRACT

Increased TMEM16A channel activities activate EGFR/STAT3/ROCK1 signaling, and ROCK1 activation by RhoA increased TMEM16A channel activities via moesin phosphorylation at T558. TMEM16A and ROCK1/moesin signaling cooperatively promotes breast cancer metastasis.



ARTICLE INFO

Article history:

Received 3 September 2020

Revised 28 January 2021

Accepted 13 March 2021

Available online 17 March 2021

ABSTRACT

Introduction: Transmembrane protein 16A (TMEM16A) is a Ca^{2+} -activated chloride channel that plays a role in cancer cell proliferation, migration, invasion, and metastasis. However, whether TMEM16A contributes to breast cancer metastasis remains unknown.

Objective: In this study, we investigated whether TMEM16A channel activation by ROCK1/moesin promotes breast cancer metastasis.

Abbreviations: ER, estrogen receptor; PR, progesterone receptor; HNSCC, head and neck squamous cell carcinoma; EGFR, epidermal growth factor receptor; STAT3, signal transducers and activators of transcription 3; FBS, fetal bovine serum; shRNAs, small hairpin RNAs; H&E, hematoxylin and eosin; IHC, immunohistochemical; TCGA, The Cancer Genome Atlas; OS, overall survival; MFS, metastasis-free survival; ROCK1, Rho-associated, coiled-coil containing protein kinase 1.

Peer review under responsibility of Cairo University.

* Corresponding author at: Department of Ion Channel Pharmacology, School of Pharmacy, China Medical University, No.77 Puhe Road, Shenyang North New Area, Shenyang 110122, China.

E-mail address: qinghuanxiao12345@163.com (Q. Xiao).

<https://doi.org/10.1016/j.jare.2021.03.005>

2090-1232/© 2021 The Authors. Published by Elsevier B.V. on behalf of Cairo University.

This is an open access article under the CC BY-NC-ND license (<http://creativecommons.org/licenses/by-nc-nd/4.0/>).

Keywords:
TMEM16A
Cl⁻ channel
Metastasis
ROCK1
Moesin

Methods: Wound healing assays and transwell migration and invasion assays were performed to study the migration and invasion of MCF-7 and T47D breast cancer cells. Western blotting was performed to evaluate the protein expression, and whole-cell patch clamp recordings were used to record TMEM16A Cl⁻ currents. A mouse model of breast cancer lung metastasis was generated by injecting MCF-7 cells via the tail vein. Metastatic nodules in the lung were assessed by hematoxylin and eosin staining. Lymph node metastasis, overall survival, and metastasis-free survival of breast cancer patients were assessed using immunohistochemistry and The Cancer Genome Atlas dataset.

Results: TMEM16A activation promoted breast cancer cell migration and invasion *in vitro* as well as breast cancer metastasis in mice. Patients with breast cancer who had higher TMEM16A levels showed greater lymph node metastasis and shorter survival. Mechanistically, TMEM16A promoted migration and invasion by activating EGFR/STAT3/ROCK1 signaling, and the role of the TMEM16A channel activity was important in this respect. ROCK1 activation by RhoA enhanced the TMEM16A channel activity via the phosphorylation of moesin at T558. The cooperative action of TMEM16A and ROCK1 was supported through clinical findings indicating that breast cancer patients with high levels of TMEM16A/ROCK1 expression showed greater lymph node metastasis and poor survival.

Conclusion: Our findings revealed a novel mechanism underlying TMEM16A-mediated breast cancer metastasis, in which ROCK1 increased TMEM16A channel activity via moesin phosphorylation and the increase in TMEM16A channel activities promoted cell migration and invasion. TMEM16A inhibition may be a novel strategy for treating breast cancer metastasis.

© 2021 The Authors. Published by Elsevier B.V. on behalf of Cairo University. This is an open access article under the CC BY-NC-ND license (<http://creativecommons.org/licenses/by-nc-nd/4.0/>).

Introduction

The transmembrane protein 16A (TMEM16A) Ca²⁺-activated Cl⁻ channel plays various physiological roles, including fluid secretion from epithelial cells, smooth muscle contraction, and transmission of nociception [1–4]. Recent studies have revealed that TMEM16A expression is upregulated in various cancers, including breast cancer [5–7], pancreatic cancer [8], and colorectal cancer [9,10]. In breast cancer, TMEM16A overexpression owing to gene amplification was shown to correlate with poor clinical outcomes [5]. Tamoxifen, a hormone therapy drug used for estrogen receptor (ER)-positive breast cancer, inhibits TMEM16A channels [3]. In our previous study, high TMEM16A expression was observed to correlate with decreased survival in patients with breast cancer not treated with tamoxifen and with increased survival in tamoxifen-treated patients [6]. Therefore, TMEM16A may serve as a biomarker for clinical outcomes and therapeutic responses to tamoxifen [11].

TMEM16A is associated with several biological processes in cancer, such as proliferation, apoptosis, migration, invasion, and metastasis, and activates multiple signaling pathways in distinct cancer types [11,12]. TMEM16A activates MAPK signaling in head and neck squamous cell carcinoma (HNSCC) [13], NF-κB signaling in glioma [14], and EGFR signaling in pancreatic cancer [8]. TMEM16A appears to preferentially activate the EGFR signaling pathway, although the downstream signaling pathways of EGFR may be different. For example, TMEM16A was shown to control Ca²⁺ signaling via EGFR in pancreatic cancer [8], and activate EGFR/AKT signaling in breast cancer [5]. TMEM16A activates the EGFR/signal transducer and activator of transcription 3 (STAT3) signaling pathway in ER-positive (ER⁺) breast cancer cells [6]. Therefore, TMEM16A can activate different signaling pathways depending on the cancer cell-specific environment [11,12].

Most studies have reported that TMEM16A promotes cell migration and invasion *in vitro* in several types of cancer, including pancreatic cancer, HNSCC, gastric cancer, and colorectal cancer [8,9,11,12,15,16]. However, whether TMEM16A promotes or inhibits cancer metastasis remains unclear. For example, TMEM16A overexpression was observed to exert an inhibitory effect on migration, invasion, and metastasis in HNSCC cells [17]. However, the metastasis-promoting effect of TMEM16A was reported in a previous study, in which increased TMEM16A expression was asso-

ciated with distant metastasis in patients with HNSCC [16]. Cao et al. reported that TMEM16A downregulation by microRNA-381 inhibited metastasis in gastric cancer [18], which suggested that TMEM16A overexpression promotes metastasis in gastric cancer. Furthermore, it was shown in an animal study that TMEM16A knockdown reduced lung metastasis of gastric cancer in mice [19].

To date, it remains unclear whether TMEM16A participates in breast cancer metastasis. The present study demonstrated that TMEM16A promoted the migration, invasion, and metastasis of breast cancer cells. In addition, patients with breast cancer with higher TMEM16A levels showed greater levels of lymph node metastasis and shorter survival. Mechanistically, increased TMEM16A channel activity promoted the expression of Rho-associated, coiled-coil-containing protein kinase 1 (ROCK1) by activating the EGFR/STAT3 signaling pathway, and ROCK1 increased TMEM16A channel activity by phosphorylating moesin at T558. Our findings suggest that TMEM16A activation by ROCK1/moesin is critical for breast cancer metastasis.

Materials and methods

Cell culture

ER⁺ and progesterone receptor (PR)-positive (PR⁺) MCF-7 and T47D breast cancer cells, normal breast MCF-10A cells, and human embryonic kidney (HEK293) cells that are used for transfection experiments were cultured in DMEM (HyClone, USA), and triple-negative MDA-MB-231 cells were cultured in Leibovitz's L-15 Medium (HyClone, USA). All cell lines were obtained from ATCC, USA. The cells were cultured in medium supplemented with fetal bovine serum (FBS, 10%) and penicillin/streptomycin (1%) at 37 °C in 5% CO₂. Cells obtained from up to ten passages were used for the subsequent experiments.

Transfection

TMEM16A-containing pEGFP-N1 plasmids were provided by Professor Uhtaek Oh [3]. TMEM16A lacking an EGFP tag was produced by introducing a stop codon at the end of the TMEM16A gene sequence. Moesin-containing pGV146-EGFP plasmids, RhoA-V14- and RhoA-19N-containing pGV147-DsRed2 plasmids, and small hairpin RNAs (shRNAs) against human TMEM16A were

constructed by Shanghai GenePharma (Shanghai, China). T558D-moesin and T558A-moesin were generated using site-directed mutagenesis. All constructs were confirmed by sequencing. Three shRNAs were constructed against TMEM16A by Shanghai GenePharma (Shanghai, China) with the following targeting sequences: shRNA1: 5'-TCACTAACTGGTCTCCAT-3'; shRNA2, 5'-ACCTGGTCAGGAAGTATTT-3'; shRNA3: 5'-TCGAGTTCAACGACAGAAA-3'. Lipofectamine 2000 (Invitrogen, USA) was used for cell transfection according to the manufacturer's instructions.

Western blotting

Western blotting was performed as previously described [6]. Briefly, after protein separation by SDS-PAGE and transfer to PVDF membranes, the membranes were treated with anti-TMEM16A antibody (1:5000; ab84915, Abcam Biotechnology, UK), anti-GFP antibody (1:3000; AE012; ABclonal Technology, China), anti-ROCK1 antibody (1:2000; ab45171; Abcam Biotechnology), anti-p-ROCK1 antibody (1:2000; ab203273; Abcam Biotechnology), anti-p-moesin antibody (1:2000; ab177943; Abcam Biotechnology), anti-moesin antibody (1:2000; ab52490; Abcam Biotechnology), anti- β -actin antibody (1:5000; ZSGB-BIO, China), and anti-GAPDH antibody (1:5000; E021010; EarthOx, USA) overnight at 4 °C, followed by treatment with secondary antibodies (dilution 1:5000; BL001A or BL003A, Biosharp, China).

Wound healing assay

MCF-7 or T47D cells (1×10^6 cells) were seeded in six-well plates. Confluent cells were gently scratched using a 200- μ L pipette tip, followed by gentle washing with PBS. After different drug treatments, images were recorded at 0–48 h using a light microscope, and the wound area was analyzed.

Transwell migration and invasion assay

An 8- μ m pore-size membrane (Corning Co., USA) was used for the migration assay. A membrane pre-coated with Matrigel (BD Biosciences, USA) was used for the invasion assay. MCF-7 or T47D cells (5×10^4) were seeded on the upper Transwell chamber (Costar 3422; Corning Co.), which was placed into the lower chamber containing the culture medium supplemented with 10% FBS. After 48 h of incubation, the cells that did not migrate or invade were removed, and the migrating or invading cells were fixed, stained in 0.2% crystal violet solution, and imaged under an inverted microscope.

Patch clamp recordings

Ca²⁺-activated Cl⁻ currents in TMEM16A-overexpressing HEK293 and T47D cells were measured using an Axopatch 200B amplifier with a Digidata 1322A digitizer (Molecular Device) [6,20]. Clampex 10 software was used for data acquisition and analysis. The standard external solution and pipette solutions with free Ca²⁺ concentrations between and 0–25 μ M were prepared as previously described [6,20,21].

Ethics statement

All experiments involving animals were conducted according to the ethical policies and procedures approved by the Ethics Committee of China Medical University, China (approval No. CMU2019300). The use of human breast cancer tissues was approved by the Ethics Committee of China Medical University (approval No. CMU2020063). Informed consent was obtained from all patients.

Mouse model of breast cancer metastasis

Female BALB/c athymic nude mice (weight: 16–20 g) were used to generate a mouse model of breast cancer lung metastasis. Ten mice were randomly assigned to two groups (n = 5 per group). Mice in the control group were injected with empty vector-transfected MCF-7 cells, and those in the TMEM16A-overexpression group were injected with TMEM16A-transfected MCF-7 cells. MCF-7 cells (2×10^6) suspended in PBS (100 μ L) were injected via the tail vein. Body weight was measured once a week. The mice were euthanized 7 weeks after injection. After sacrifice, the lungs were harvested, fixed, and embedded in paraffin. Serial lung tissue sections were stained with hematoxylin and eosin (H&E). Metastatic nodules in the lung specimens were counted under a light microscope.

Immunohistochemistry

ER⁺/PR⁺/HER2⁻ breast cancer tissue samples (n = 72) obtained from the First Affiliated Hospital of China Medical University were used for immunohistochemical detection of TMEM16A and ROCK1. Clinical information, including lymph node metastasis and ER, PR, and HER2 status, was obtained retrospectively from the medical records. All breast cancers were diagnosed by histopathology.

Immunohistochemical analysis was performed as previously described [6]. Briefly, tissue sections (4- μ m thick) were treated with anti-TMEM16A antibody (1:400), anti-ROCK1 antibody (1:150), IgG (1:150; bs-0295P; Beijing Biosynthesis Biotechnology Inc, China), or no antibodies in controls at 4 °C, followed by treatment with biotinylated secondary antibodies (1:3000; Fuzhou Maixin, China) and 3, 3'-diaminobenzidine (DAB) at room temperature. The primary antibodies were purchased from Abcam Biotechnology.

Statistical analysis

The Cancer Genome Atlas (TCGA) data for the RNA expression of ROCK1 and TMEM16A were used for survival analysis of patients with breast cancer. Survival was evaluated using Kaplan–Meier curves and compared statistically using log-rank tests. Overall survival (OS) was defined as the duration between cancer diagnosis and death. Metastasis-free survival (MFS) was defined as the duration between cancer diagnosis and the occurrence of metastasis or death.

Clampfit10 was used to analyze the Cl⁻ current traces. Statistical analysis was performed using SPSS software. Differences with $p < 0.05$ were considered statistically significant. The differences between two groups were compared using Student's *t*-test. One-way ANOVA was performed to determine the differences among more than two groups, followed by the post-hoc Bonferroni test for multiple comparisons. Chi-square tests were performed to compare the difference in the distribution of lymph node metastasis between the groups.

Results

TMEM16A overexpression promotes breast cancer cell migration, invasion, and metastasis

TMEM16A expression was relatively high in ER⁺/PR⁺/HER2⁻ MCF-7 and T47D cells, whereas it was relatively low in triple-negative MDA-MB-231 cells and MCF-10A cells (normal breast cells) (Fig. S1). Western blotting results confirmed that TMEM16A knockdown by TMEM16A-shRNA2 treatment decreased TMEM16A expression (Fig. S2A, B), whereas TMEM16A overexpression by

transfection of TMEM16A-containing plasmids increased TMEM16A expression in MCF-7 cells and in T47D cells (Fig. S2C, D). TMEM16A knockdown by TMEM16A-shRNA2 treatment inhibited migration and invasion, whereas TMEM16A overexpression promoted migration and invasion in MCF-7 cells (Fig. 1). Similarly, TMEM16A knockdown inhibited, and TMEM16A overexpression promoted migration and invasion in T47D cells (Fig. S3). These findings suggested that TMEM16A promoted breast cancer cell migration and invasion.

The role of TMEM16A in breast cancer cell metastasis was examined *in vivo* in nude mice by injecting TMEM16A-overexpressing MCF-7 cells via the tail vein. The body weight of mice increased gradually within 6 weeks of injection of control or TMEM16A-overexpressing MCF-7 cells. At each time point, the body weight gain did not differ significantly between mice injected with control and TMEM16A-overexpressing cells, although mice injected with TMEM16A-overexpressing MCF-7 cells had a marginally lower body weight than control mice (Fig. 2A). The number of metastatic nodules in the lung was greater in mice injected with TMEM16A-overexpressing MCF-7 cells than in control mice (Fig. 2B, C). These findings suggested that TMEM16A overexpression promoted breast cancer metastasis *in vivo*.

We then analyzed the association of lymph node metastasis with TMEM16A expression in patients with ER⁺/PR⁺/HER2⁻ breast cancer (n = 72) using immunohistochemistry (Fig. 2D and Fig. S4). Table S1 summarizes the clinicopathological characteristics of 72 patients with ER⁺/PR⁺/HER2⁻ breast cancer. Lymph node metastasis was observed more frequently in patients with high TMEM16A expression (70.8%, 17/24 patients) than in those with low TMEM16A expression (43.8%, 21/48) (p = 0.030, Fig. 2E). Of the patients with ER⁺/PR⁺/HER2⁻ breast cancer (n = 706) in the TCGA dataset, lymph node metastasis was observed frequently in patients with high TMEM16A mRNA expression (62.6%, 137/219 patients) than in those with low TMEM16A mRNA expression (54.0%, 263/487 patients) (p = 0.034, Fig. 2F). We selected patients who did not undergo any treatment (n = 181) from the TCGA dataset for survival analysis for excluding the possible effect of chemotherapy or hormone therapy on the survival of patients. High TMEM16A expression levels correlated significantly with shorter MFS (p = 0.008, Fig. 2G) and OS (p = 0.004, Fig. 2H) in patients who did not undergo any treatment.

TMEM16A promotes migration and invasion by activating EGFR/STAT3/ROCK1 signaling

ROCK1 has been shown to regulate cell motility and promote cancer cell migration, invasion, and metastasis [22]. Our previous study showed that TMEM16A activates EGFR/STAT3 signaling in breast cancer [6]. EGFR signaling activation by EGF significantly increased ROCK1 expression in MCF-7 cells (Fig. S5A). In addition, a positive correlation of ROCK1 expression with EGFR expression (n = 181, r = 0.4012, p < 0.0001) and STAT3 expression (n = 181, r = 0.5346, p < 0.0001) was observed in patients with breast cancer from the TCGA dataset (Fig. S5B, C). These findings suggest that EGFR/STAT3 signaling activation promoted ROCK1 expression in breast cancer. Moreover, TMEM16A knockdown significantly inhibited ROCK1 expression, whereas TMEM16A overexpression enhanced ROCK1 expression (Fig. 3A, B). The TMEM16A overexpression-induced upregulation of ROCK1 expression was inhibited by gefitinib or JSI-124, which inhibit EGFR and STAT3, respectively (Fig. 3C-F). These findings suggested that TMEM16A upregulated ROCK1 expression by activating EGFR/STAT3 signaling.

We explored whether TMEM16A promotes migration and invasion by activating EGFR/STAT3/ROCK1 signaling. TMEM16A overexpression-induced migration and invasion was significantly

inhibited by gefitinib, JSI-124, and the ROCK inhibitor Y-27632 in both T47D and MCF-7 cells (Fig. 4 and Fig. S6). Therefore, TMEM16A promoted the migration and invasion of breast cancer cells by activating the EGFR/STAT3/ROCK1 signaling pathway.

Increased TMEM16A channel activity promotes cell migration and invasion

We previously observed that TMEM16A knockdown inhibited Ca²⁺-activated Cl⁻ currents in T47D cells [6]. Consistent with our previous results, the TMEM16A inhibitor T16Ainh-A01 significantly inhibited TMEM16A Ca²⁺-activated Cl⁻ current in T47D cells (Fig. S7). In addition, T16Ainh-A01 significantly blocked TMEM16A overexpression-induced migration and invasion in T47D cells (Fig. 5A, B). Moreover, compared to wild-type (WT)-TMEM16A overexpression, the overexpression of $\Delta_{444}EEEEAVKD_{452}$ -TMEM16A mutants, which exhibit decreased channel activity [20], inhibited ROCK1 expression (Fig. 5C) as well as migration and invasion of T47D cells (Fig. 5D, E).

ROCK1 promotes TMEM16A channel activity by phosphorylating moesin

ROCK1 is known to phosphorylate moesin at T558, which is a critical step for maintaining moesin in an active form for membrane localization [23]. We investigated whether ROCK1 promoted TMEM16A channel activity in T47D cells by phosphorylating moesin at T558. The Ca²⁺-activated Cl⁻ currents were significantly inhibited by the ROCK inhibitor Y-27632 (Fig. 6A-C), suggesting that ROCK1 promoted TMEM16A currents in T47D cells. Compared to the overexpression of constitutively inactive RhoA mutants (RhoA-19 N), the overexpression of constitutively active RhoA mutants (RhoA-V14) resulted in ROCK1 activation and moesin phosphorylation at T558 (Fig. 6D). The overexpression of RhoA-V14 mutants significantly promoted Ca²⁺-activated Cl⁻ currents (Fig. 6E, F), suggesting that ROCK1 activation by RhoA promoted TMEM16A activation in T47D cells. Compared to non-phosphorylatable T558A-moesin mutant overexpression, phosphomimetic T558D-moesin mutant overexpression significantly increased TMEM16A currents in T47D (Fig. 6G, H) and HEK293 cells transfected with TMEM16A-containing plasmids (Fig. 6I, J), suggesting that moesin phosphorylation at T558 enhanced TMEM16A channel activity. Collectively, these findings indicate that ROCK1 promotes TMEM16A channel activity via moesin phosphorylation.

High TMEM16A/ROCK1 expression correlates with breast cancer metastasis

The association of combined TMEM16A/ROCK1 expression with lymph node metastasis was studied to investigate the effect of TMEM16A/ROCK1 expression on breast cancer metastasis. Lymph node metastasis occurred more frequently in patients with high TMEM16A/ROCK1 expression (76.5%, 13/17 patients) than in those with low TMEM16A/ROCK1 expression (29.4%, 5/17) (p = 0.015; Fig. S8A, B). Similarly, using the TCGA dataset, we observed that the frequency of occurrence of lymph node metastasis was significantly greater in patients with breast cancer with high TMEM16A/ROCK1 expression (63.6%, 103/162) than in those with low TMEM16A/ROCK1 expression (49.5%, 99/200) (p = 0.007, Fig. S8C). In addition, high TMEM16A/ROCK1 expression correlated with a shorter MFS (p = 0.075, Fig. S8D) and OS (p = 0.037, Fig. S8E) in patients with breast cancer who did not undergo any treatment.

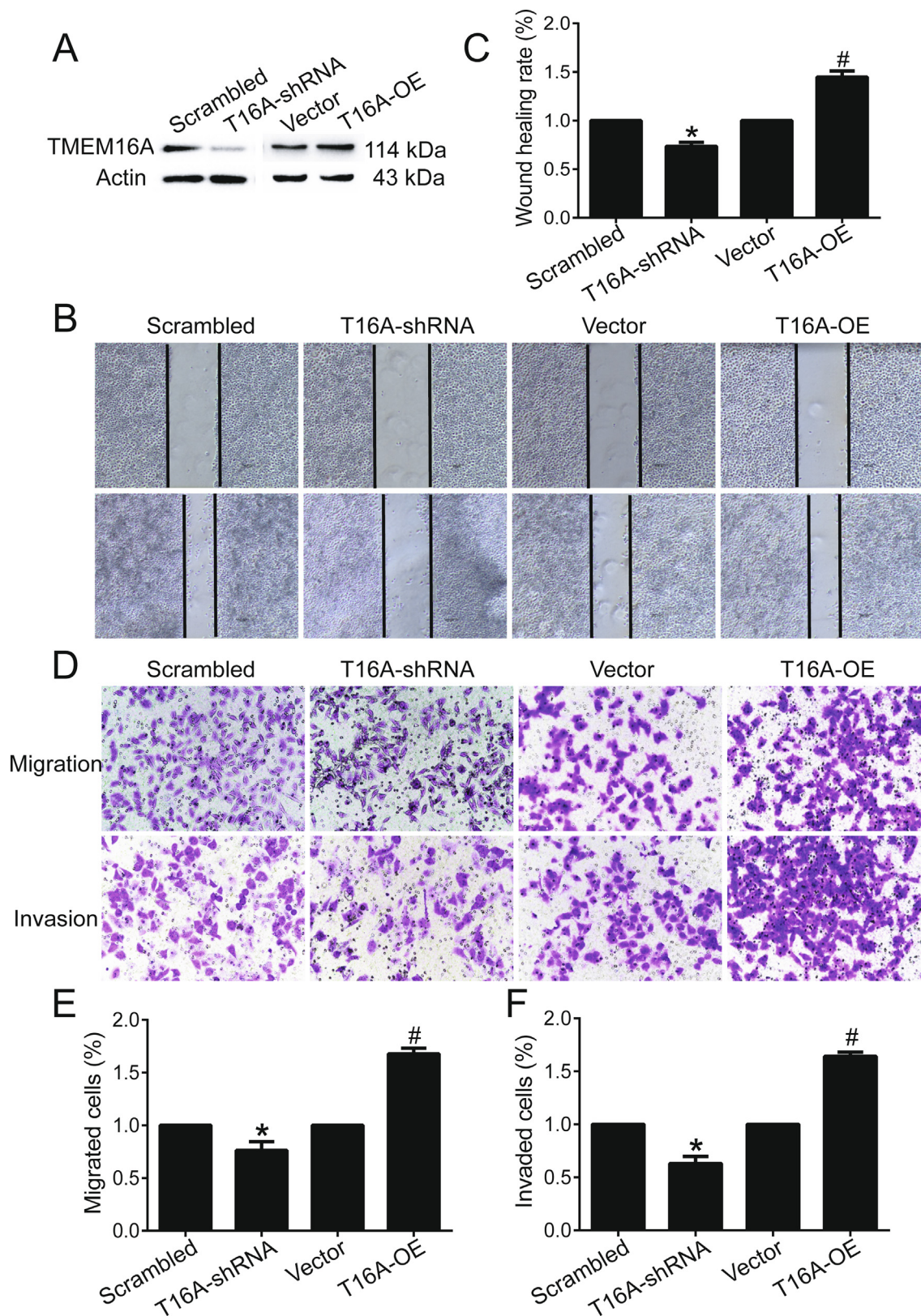


Fig. 1. TMEM16A promoted the migration and invasion of MCF-7 cells. **A.** TMEM16A protein expression in MCF-7 cells treated with scrambled shRNA and TMEM16A-shRNA (T16A-shRNA) or empty vector and TMEM16A-containing plasmids (T16A-OE). **B.** The wound healing assay showed the migration of MCF-7 cells treated with scrambled shRNA and T16A-shRNA or empty vectors and T16A-OE plasmids. **C.** Quantification of the results of the wound healing assay shown in B. n = 3. *p < 0.05 vs scrambled; #p < 0.05 vs vector. **D.** Transwell assays indicating migration (**top**) and invasion (**bottom**) of MCF-7 cells treated with scrambled shRNA and T16A-shRNA, or empty vector and T16A-OE plasmids. **E, F.** Quantification results for cell migration (**E**) and invasion (**F**) shown in D. n = 3. *p < 0.05 vs scrambled; #p < 0.05 vs vector.

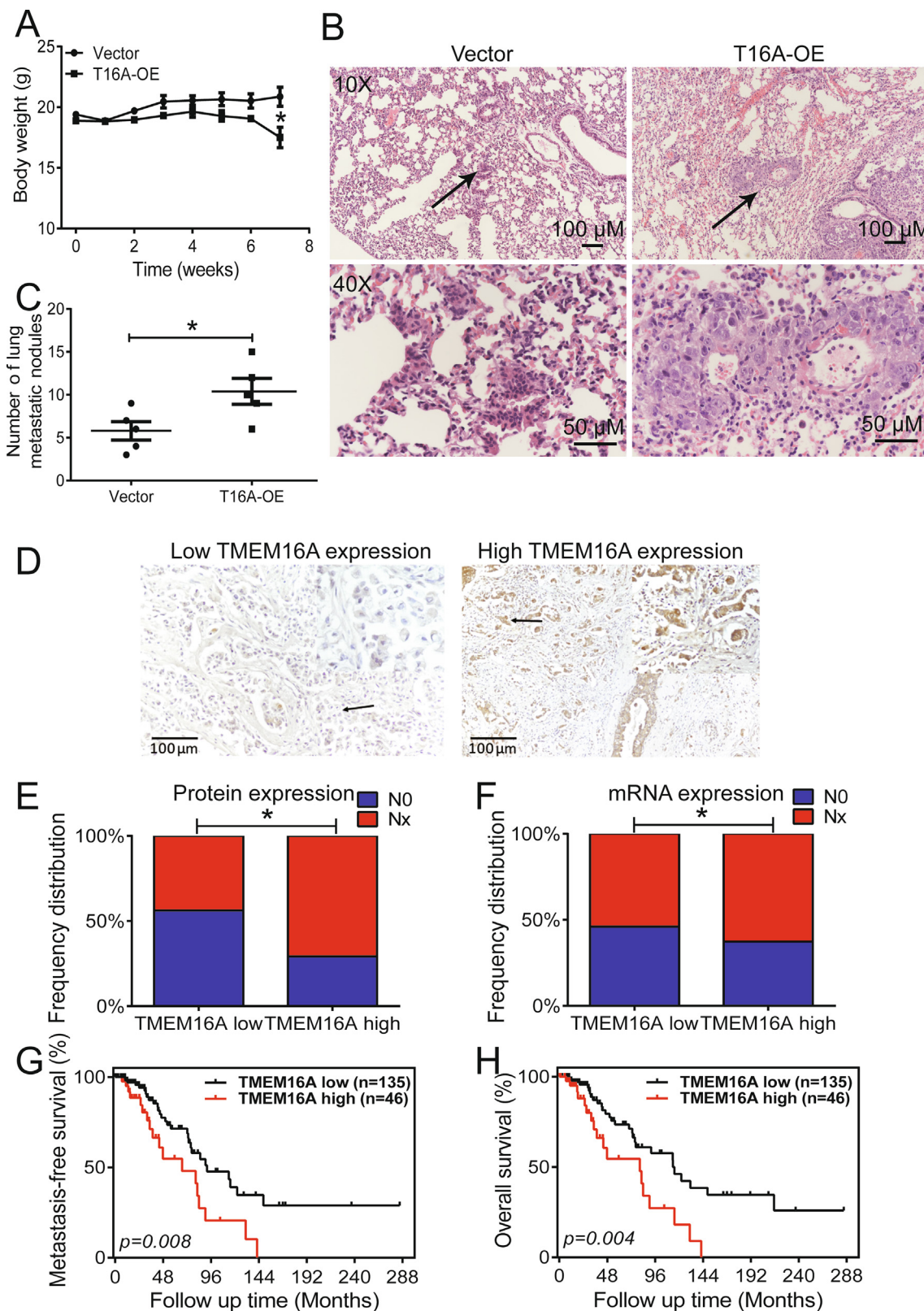


Fig. 2. TMEM16A overexpression promoted breast cancer lung metastasis in mice. **A.** Body weight of mice after intravenous injection of MCF-7 cells transfected with empty vector or T16A-OE plasmids. $n = 5$. * $p < 0.05$ vs vector. **B.** Representative H&E staining images depicting metastatic nodules in the lung at low magnification ($\times 10$) (top) and high magnification ($\times 40$) (bottom). The arrows indicate the magnified regions. Scale bar: 100 (top) and 50 μm (bottom). **C.** The number of metastatic nodules in the lung of mice carrying vector- or T16A-OE-transfected MCF-7 cells. $n = 5$. * $p < 0.05$. **D.** Immunohistochemical images for low (left) and high (right) TMEM16A expression in breast cancer tissues. Magnification: $\times 40$. Scale bar: 100 μm . Immunohistochemical results were scored (a total of 0–300) based on the intensity of immunoreactivity (0–3) and the percentage of TMEM16A-positive cells (0–100). Tumors with IHC score > 150 or ≤ 150 was defined as tumors with high or low expression of TMEM16A, respectively. **E, F.** Frequency distribution of lymph node metastasis in patients with breast cancer with low and high expression of TMEM16A protein (E) and mRNA (F) based on immunohistochemical analysis (E) and TCGA dataset (F). $p = 0.030$ (E) and $p = 0.034$ (F). **G, H.** Survival curves depicting the association of TMEM16A expression with metastasis-free survival (G) and overall survival (H) in patients with breast cancer who did not undergo treatment ($n = 181$). $p = 0.008$ (G) and $p = 0.004$ (H).

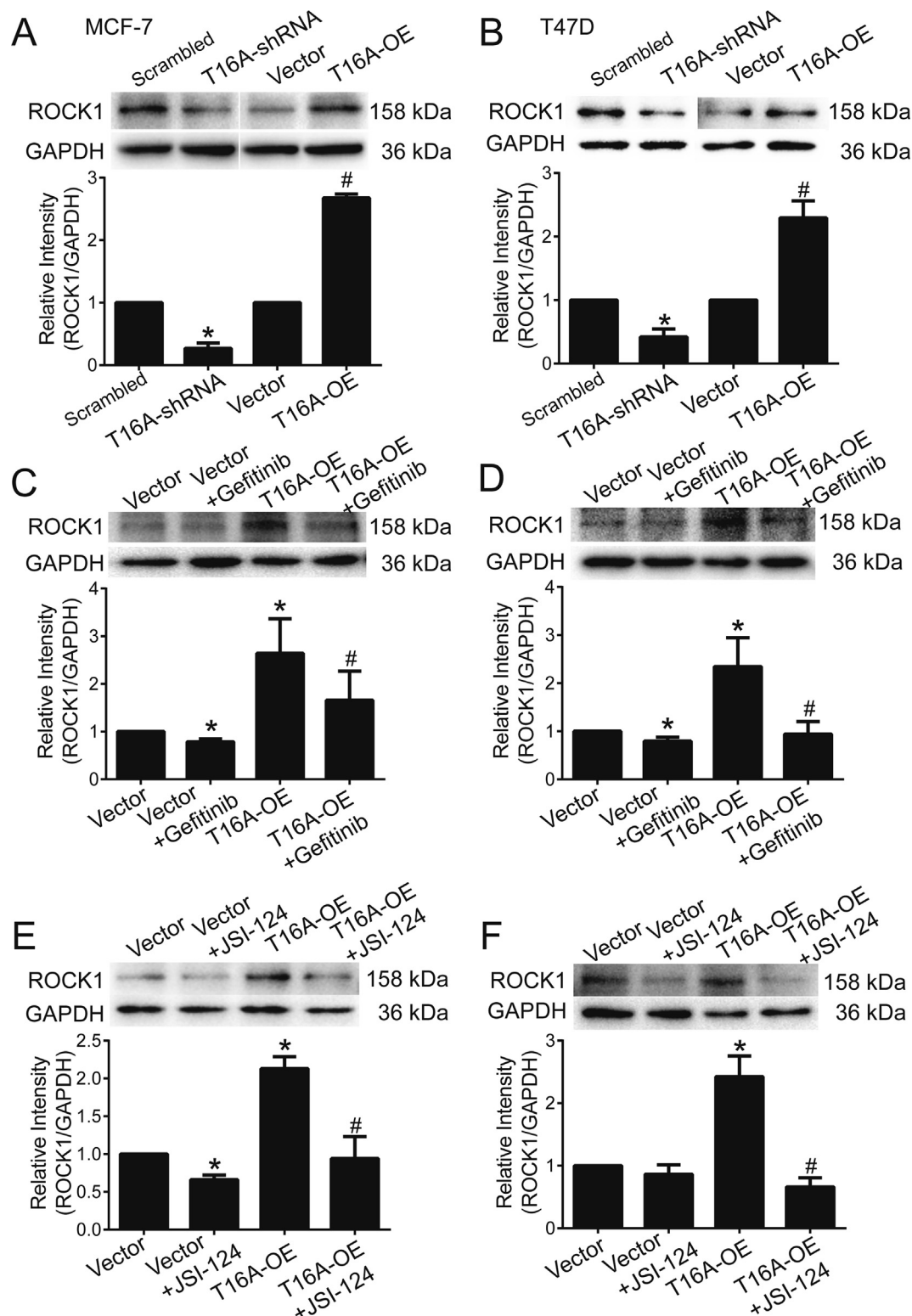


Fig. 3. TMEM16A promoted ROCK1 expression by activating EGFR/STAT3 signaling. **A, B.** ROCK1 protein expression in MCF-7 (**A**) and T47D cells (**B**) treated with scrambled shRNA and T16A-shRNA or empty vector and T16A-OE plasmids. *n* = 3. **p* < 0.05 vs scrambled shRNA, #*p* < 0.05 vs vector. **C-F.** ROCK1 protein expression in MCF-7 (**C, E**) and T47D cells (**D, F**) transfected with empty vector or T16A-OE plasmids in the absence or presence of gefitinib (1 μM) (**C, D**) or JSI-124 (0.1 μM) (**E, F**). *n* = 3. **p* < 0.05 vs vector, #*p* < 0.05 vs T16A-OE.

Discussion

TMEM16A is known to contribute to cell proliferation, migration, invasion, and metastasis in multiple cancer types [11,12]. Sev-

eral studies have demonstrated that TMEM16A promotes the proliferation of breast cancer cells and tumor growth in mice [5,6]. However, the precise role of TMEM16A in breast cancer migration, invasion, and metastasis remains unclear. Here, our

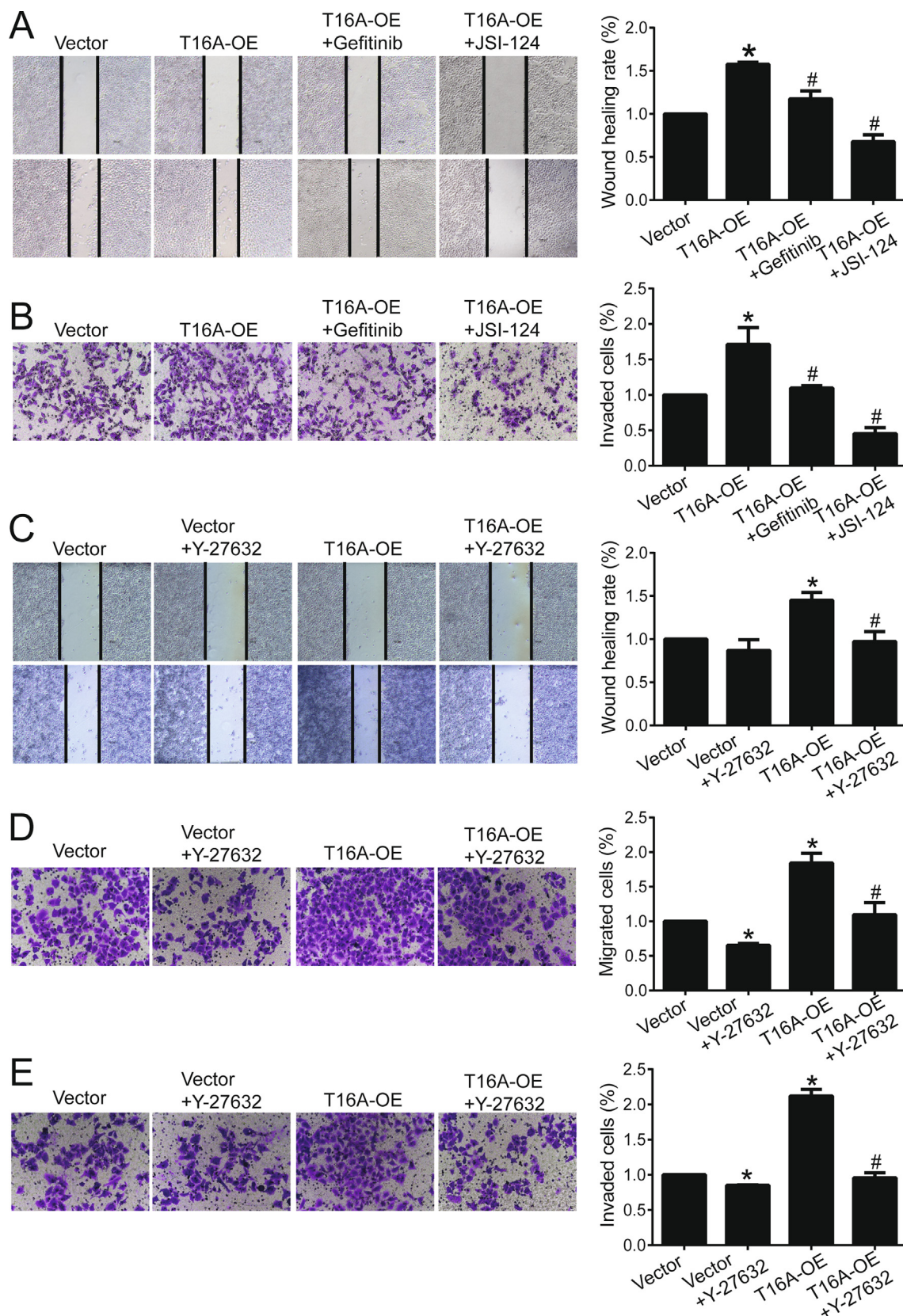


Fig. 4. TMEM16A overexpression promoted migration and invasion of T47D cells via the activation of EGFR/STAT3/ROCK1 signaling. **A, B.** Wound healing assay (**A**) and transwell assay (**B**) showed the migration (**A**) or invasion (**B**) of T47D cells treated with empty vector or T16A-OE plasmids in the absence or presence of gefitinib (1 μM) or JSI-124 (0.1 μM). n = 3. *p < 0.05 vs vector; #p < 0.05 vs T16A-OE. **C.** Wound healing assay showed the migration of T47D cells treated with empty vector or T16A-OE plasmids in the absence or presence of Y-27632 (10 μM). n = 3. *p < 0.05 vs vector; #p < 0.05 vs T16A-OE. **D, E.** Transwell assay showed the migration (**D**) and invasion (**E**) of T47D cells treated with empty vector or T16A-OE plasmids in the absence or presence of Y-27632 (10 μM). n = 3. *p < 0.05 vs vector; #p < 0.05 vs T16A-OE.

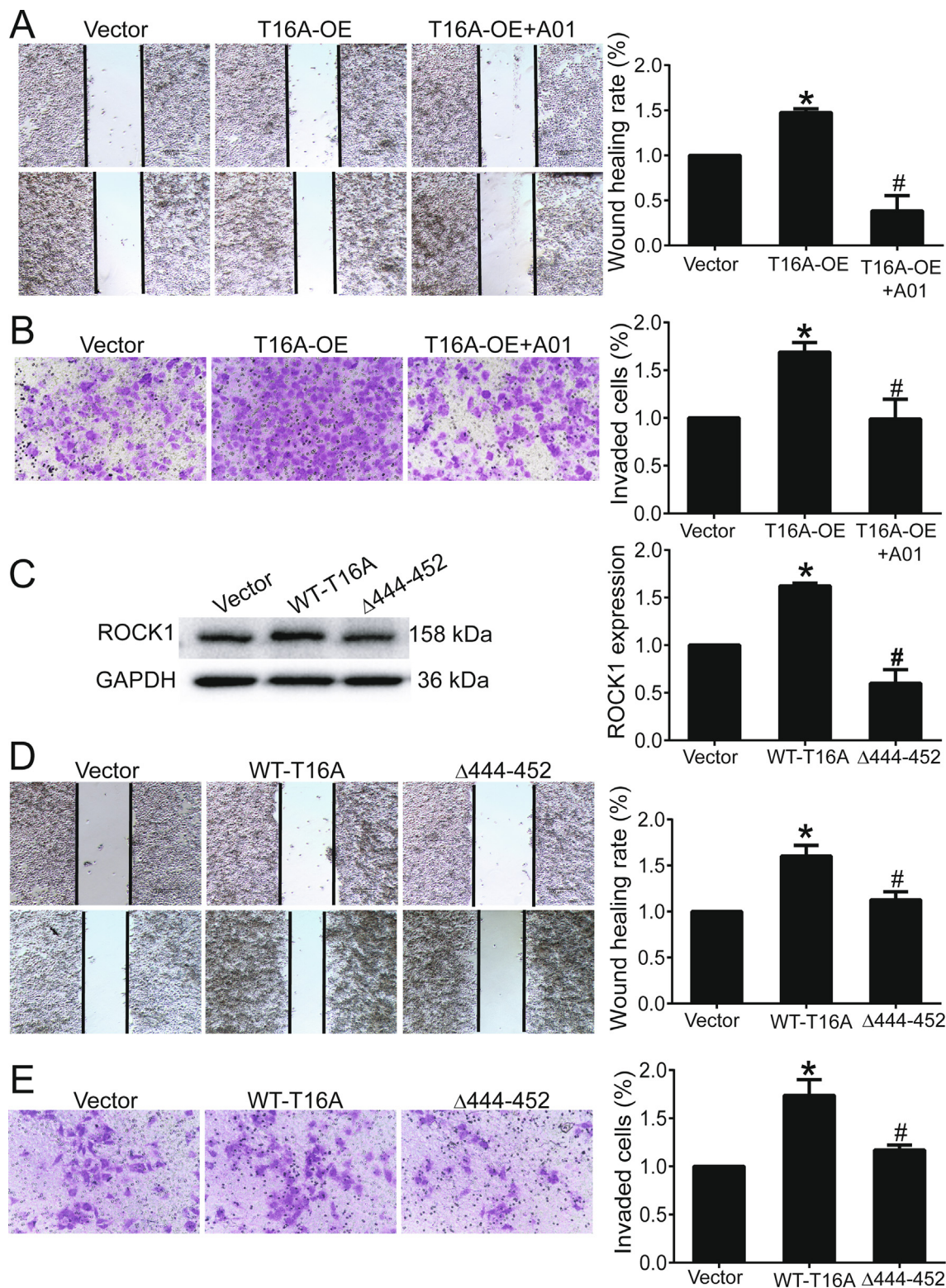


Fig. 5. Inhibition of TMEM16A channel activity reduced the migration and invasion of T47D cells. **A, B.** Wound healing assay (**A**) and transwell assay (**B**) showed the migration (**A**) and invasion (**B**) of T47D cells treated with empty vector, T16A-OE plasmids, and T16A-OE + T16Ainh-A01 (20 μ M). $n = 3$. * $p < 0.05$ vs vector; # $p < 0.05$ vs T16A-OE. **C.** ROCK1 protein expression in T47D cells transfected with empty vector or plasmids containing WT-TMEM16A/ $\Delta 444$ EEEEAVKD₄₅₂-TMEM16A ($\Delta 444-452$) mutants. $n = 3$. * $p < 0.05$ vs vector, # $p < 0.05$ vs WT-TMEM16A. **D, E.** Wound healing assay (**D**) and transwell assay (**E**) showed the migration (**D**) and invasion (**E**) of T47D cells treated with empty vector or plasmids containing WT TMEM16A or $\Delta 444-452$ mutants. $n = 3$. * $p < 0.05$ vs vector; # $p < 0.05$ vs WT-TMEM16A.

results demonstrated that TMEM16A overexpression promoted migration, invasion, and metastasis in breast cancer cells. Increased TMEM16A channel activity promoted ROCK1 expression

by activating EGFR/STAT3 signaling. ROCK1 increased TMEM16A channel activity by phosphorylating moesin at T558 (Fig. S9). Therefore, TMEM16A and ROCK1 mutually activate each other

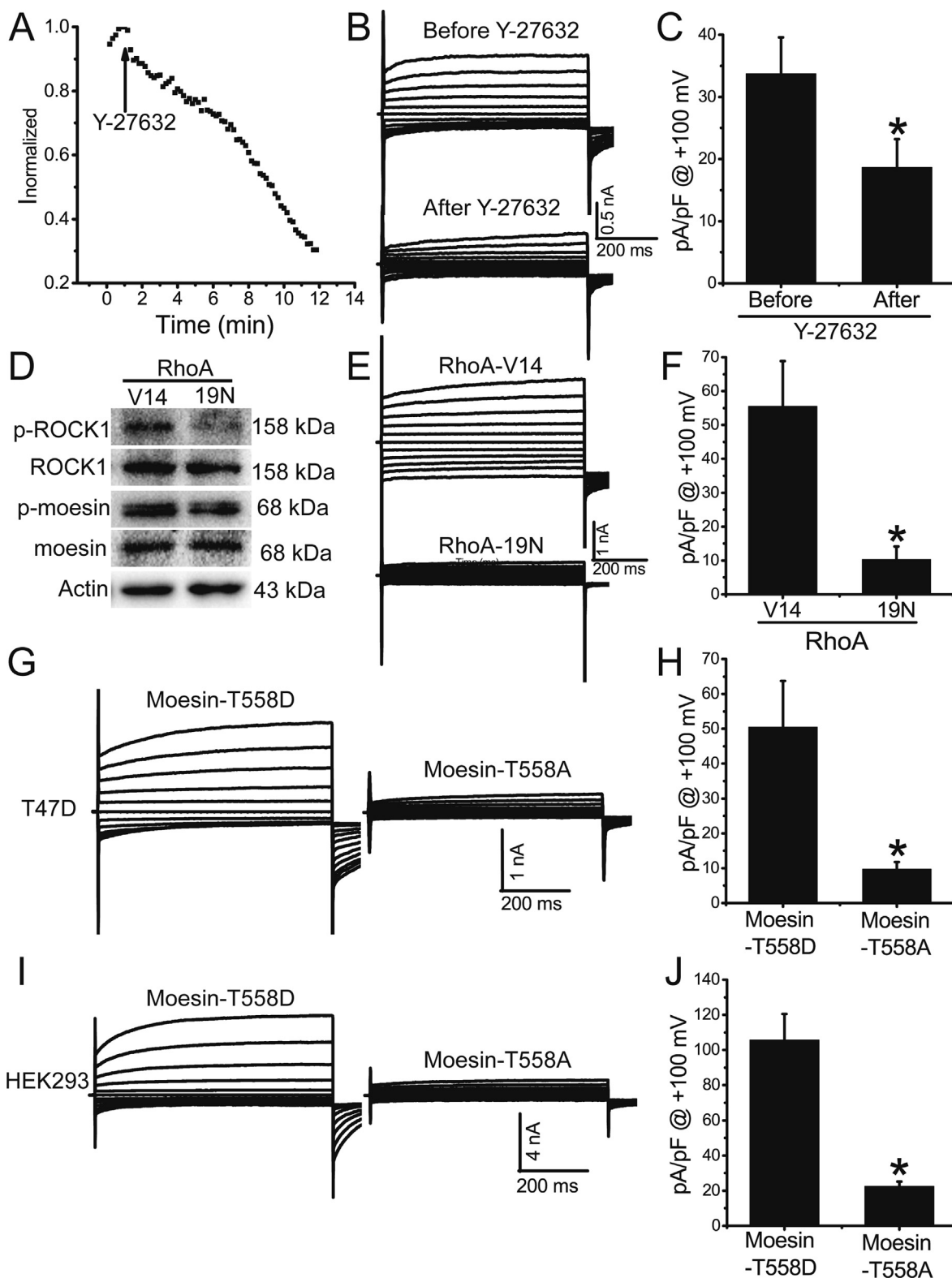


Fig. 6. ROCK1 promoted TMEM16A channel activity by phosphorylating moesin at T558. **A.** Time course of Ca^{2+} ($1 \mu\text{M}$)-activated Cl^- currents in T47D cells treated with the ROCK inhibitor Y-27632 ($10 \mu\text{M}$). Voltage ramps 750 ms in duration were induced at 10-s intervals. The arrow indicates treatment with Y-27632. The currents were normalized to the initial values of current prior to Y-27632 treatment. **B.** Representative TMEM16A currents before (**top**) and after (**bottom**) Y-27632 treatment. The cells were voltage-clamped with a 750-ms voltage step from -100 mV to $+100 \text{ mV}$ in 20 mV increments. **C.** Mean current densities at $+100 \text{ mV}$ in T47D cells before and after Y-27632 treatment. $n = 5$ cells. * $p < 0.05$ vs before treatment. **D.** Expression of p-ROCK1, ROCK1, p-moesin (T558), and moesin in T47D cells overexpressing RhoA-V14 and RhoA-19 N mutants. **E.** Representative TMEM16A currents in T47D cells transfected with plasmids containing RhoA-V14 and RhoA-19 N mutants. $n = 5-6$; * $p < 0.05$. **F.** Mean current densities at $+100 \text{ mV}$ in T47D cells treated with RhoA-V14 and RhoA-19 N mutants. $n = 5-6$; * $p < 0.05$. **G, I.** Representative TMEM16A currents in response to activation by $1 \mu\text{M}$ Ca^{2+} in T47D cells (**G**) transfected with plasmids containing T558D-moesin or T558A-moesin mutants or in HEK293 cells (**I**) cotransfected with plasmids containing TMEM16A and T558D-moesin or T558A-moesin mutants. **H, J.** Mean current densities at $+100 \text{ mV}$ in T47D (**H**) and HEK293 cells (**J**). $n = 4-5$; * $p < 0.05$.

and cooperatively promote breast cancer cell migration, invasion, and metastasis. The cooperative role of TMEM16A and ROCK1 in metastasis was further supported by evidence from the survival analysis, which showed that high TMEM16A/ROCK1 expression correlated with decreased survival among patients with breast cancer. Our findings demonstrated that TMEM16A activation by ROCK1/moesin promotes breast cancer migration, invasion, and metastasis.

The mechanisms underlying TMEM16A overexpression include gene amplification, EGFR signaling regulation, and epigenetic regulation by histone deacetylase [5,6,11,24]. TMEM16A is expressed in approximately 80% of breast cancers [5,7]. Since approximately 70% of breast cancers are ER- and PR-positive, it is expected that TMEM16A is primarily expressed in these breast cancer types. In the present study, high TMEM16A expression correlated with lymph node metastasis and decreased survival in ER⁺/PR⁺ breast cancer, suggesting that TMEM16A overexpression may promote breast cancer metastasis. Consistently, TMEM16A promoted migration and invasion of breast cancer cells, and enhanced breast cancer metastasis in a mouse model of lung metastasis. Furthermore, the TMEM16A shRNAs or inhibitors suppressed cell migration and invasion. Therefore, TMEM16A inhibition might be an effective strategy for treating breast cancer metastasis.

ROCK1 promotes migration, invasion, and metastasis in several cancer types [22,25]. TMEM16A activates the EGFR signaling pathway [5,6], which then contributes to breast cancer metastasis [26,27]. In a previous study, we showed that TMEM16A activated EGFR/STAT3 signaling [6]. Here, we further observed that TMEM16A upregulated ROCK1 expression by activating EGFR/STAT3 signaling. ROCK1 expression upregulation in response to EGFR/STAT3 signaling activation was confirmed by the finding that EGF promoted ROCK1 expression in breast cancer cells, and there was a positive correlation between ROCK1 expression and EGFR/STAT3 expression in human breast cancer tissues. Furthermore, EGFR/STAT3/ROCK1 signaling inhibition significantly blocked TMEM16A-mediated migration and invasion, suggesting that ROCK1 is important for TMEM16A-mediated breast cancer metastasis. However, the process by which EGFR/STAT3 signaling promotes ROCK1 expression in breast cancer cells remains unclear. Further studies are necessary to investigate the mechanisms by which TMEM16A/EGFR/STAT3 signaling promotes ROCK1 expression in breast cancer cells.

As a serine-threonine kinase, ROCK1 regulates several downstream targets that are involved in the regulation of dynamic changes in the actin cytoskeleton during cancer cell migration, invasion, and metastasis [22]. Moesin can be activated by ROCK1 via T558 phosphorylation [23,28]. Reportedly, moesin facilitates breast cancer metastasis [29], and its expression was shown to correlate with lymph node metastasis and decreased survival in ER⁺ breast cancer [30]. Notably, moesin has been observed to interact directly with TMEM16A and promote TMEM16A channel activity when overexpressed in HEK293 cells [31]. Our results showed that T558-phosphorylated moesin promoted TMEM16A channel activity in breast cancer cells. The activation of ROCK1 by RhoA increased TMEM16A channel activity owing to the phosphorylation of moesin at T558 in breast cancer cells. Furthermore, increased TMEM16A channel activity was observed to be critical for the TMEM16A-induced migration and invasion of breast cancer cells, as indicated by the finding that the inhibition of TMEM16A channel activity by TMEM16A inhibitors or in Δ_{444} EEEEAVKD₄₅₂-TMEM16A mutants reduced cell migration and invasion. Therefore, increased TMEM16A channel activity owing to ROCK1-mediated moesin phosphorylation promotes breast cancer metastasis.

Increased TMEM16A channel activity has been shown to be important for TMEM16A-mediated EGFR activation in breast cancer [6,32]. Our previous study showed that the overexpression of

Δ_{444} EEEEAVKD₄₅₂-TMEM16A mutants inhibited WT TMEM16A-induced EGFR/STAT3 signaling activation [6]. The findings from the present study further revealed that Δ_{444} EEEEAVKD₄₅₂-TMEM16A mutants inhibited ROCK1 expression induced by WT TMEM16A, suggesting that increased TMEM16A channel activity further promoted ROCK1 expression via EGFR/STAT3 signaling activation. Consequently, ROCK1 activation by RhoA increased TMEM16A channel activity via moesin phosphorylation in breast cancer cells. Therefore, in TMEM16A-overexpressing breast cancer cells, increased TMEM16A activity may induce high levels of ROCK1 expression via EGFR/STAT3 signaling activation, and ROCK1 may further promote TMEM16A activity via moesin phosphorylation (Fig. S9). Therefore, the mutual activation mechanism indicates that TMEM16A and ROCK1/moesin may cooperatively promote breast cancer metastasis.

Ion fluxes via ion channels are associated with changes in water content, and therefore, regulate morphological changes during cancer cell migration, invasion, and metastasis [33]. Several studies have shown that TMEM16A overexpression affects morphological changes and regulates the migration, invasion, and metastasis of cancer cells [16,17,34]. The present study revealed that increased TMEM16A channel activity is a critical factor, and Cl⁻ fluxes via TMEM16A channels may contribute to morphological changes during breast cancer cell migration, invasion, and metastasis. Furthermore, morphological changes in cancer cells require drastic reorganization of the actin cytoskeleton, and ROCK1 and moesin play an important role in this process [35–37]. Moesin, which functions as a cross-linker between membrane proteins and the actin cytoskeleton [23], can directly bind to TMEM16A [31]. We further observed that increased TMEM16A activity promoted ROCK1 expression, and ROCK1 increased moesin phosphorylation, which also promoted TMEM16A channel activity (Fig. S9). Therefore, TMEM16A and ROCK1/moesin regulate cellular morphological changes in coordination, and promote cancer cell migration, invasion, and metastasis. Further studies are necessary to investigate the mechanisms by which TMEM16A and ROCK1/moesin promote migration, invasion, and metastasis in breast cancer.

Conclusions

In summary, the present study demonstrated that increased TMEM16A channel activity promotes breast cancer cell migration, invasion, and metastasis. Moesin phosphorylation by ROCK1 increased TMEM16A channel activity, which consequently promoted ROCK1 expression through the activation of EGFR/STAT3 signaling (Fig. S9). Our results suggest that TMEM16A and ROCK1/moesin may regulate breast cancer metastasis in a coordinated manner. Therefore, TMEM16A may serve as a novel target in the treatment of breast cancer metastasis.

Compliance with Ethics Requirements

All Institutional and National Guidelines for the care and use of animals (fisheries) were followed.

All procedures followed were in accordance with the ethical standards of the responsible committee on human experimentation (institutional and national) and with the Helsinki Declaration of 1975, as revised in 2008 (5). Informed consent was obtained from all patients for being included in the study.

Declaration of Competing Interest

The authors declare that they have no known competing financial interests or personal relationships that could have appeared to influence the work reported in this paper.

Acknowledgements

This work was supported by grants from the National Natural Science Foundation of China (No. 81572613 and No. 31371145 to Qinghuan Xiao; No. 81702611 to Hui Wang; No. 81802659 to Mei Liu) and the China Postdoctoral Science Foundation (No. 2019M651177 to Hui Wang; No. 2018M641738 to Mei Liu).

Appendix A. Supplementary material

Supplementary data to this article can be found online at <https://doi.org/10.1016/j.jare.2021.03.005>.

References

- Caputo A, Caci E, Ferrera L, Pedemonte N, Barsanti C, Sondo E, Pfeffer U, Ravazzolo R, Zegarra-Moran O, Galiotta LJ. TMEM16A, a membrane protein associated with calcium-dependent chloride channel activity. *Science* 2008;322(5901):590–4.
- Schroeder BC, Cheng T, Jan YN, Jan LY. Expression cloning of TMEM16A as a calcium-activated chloride channel subunit. *Cell* 2008;134(6):1019–29.
- Yang YD, Cho H, Koo JY, Tak MH, Cho Y, Shim W-S, Park SP, Lee J, Lee B, Kim B-M, Raouf R, Shin YK, Oh U. TMEM16A confers receptor-activated calcium-dependent chloride conductance. *Nature* 2008;455(7217):1210–5.
- Pedemonte N, Galiotta LJ. Structure and function of TMEM16 proteins (anoctamins). *Physiol Rev* 2014;94(2):419–59.
- Britschgi A, Bill A, Brinkhaus H, Rothwell C, Clay I, Duss S, et al. Calcium-activated chloride channel ANO1 promotes breast cancer progression by activating EGFR and CAMK signaling. *PNAS* 2013;110(11):E1026–34.
- Wang H, Yao F, Luo S, Ma Ke, Liu M, Bai L, et al. A mutual activation loop between the Ca²⁺-activated chloride channel TMEM16A and EGFR/STAT3 signaling promotes breast cancer tumorigenesis. *Cancer Lett* 2019;455:48–59.
- Wu H, Guan S, Sun M, Yu Z, Zhao L, He M, et al. Ano1/TMEM16A overexpression is associated with good prognosis in PR-positive or HER2-negative breast cancer patients following tamoxifen treatment. *PLoS One* 2015;10. doi: <https://doi.org/10.1371/journal.pone.0126128>.
- Crottès D, Lin Y-H, Peters CJ, Gilchrist JM, Wiita AP, Jan YN, Jan LY. TMEM16A controls EGF-induced calcium signaling implicated in pancreatic cancer prognosis. *PNAS* 2019;116(26):13026–35.
- Sui Y, Sun M, Wu F, Yang L, Di W, Zhang G, et al. Inhibition of TMEM16A expression suppresses growth and invasion in human colorectal cancer cells. *PLoS One* 2014;9. doi: <https://doi.org/10.1371/journal.pone.0115443>.
- Jiang Y, Cai Y, Shao W, Li F, Guan Z, Zhou Y, et al. MicroRNA144 suppresses aggressive phenotypes of tumor cells by targeting ANO1 in colorectal cancer. *Oncol Rep* 2019;41:2361–70. doi: <https://doi.org/10.3892/or.2019.7025>.
- Wang H, Zou L, Ma Ke, Yu J, Wu H, Wei M, et al. Cell-specific mechanisms of TMEM16A Ca²⁺-activated chloride channel in cancer. *Mol Cancer* 2017;16(1). doi: <https://doi.org/10.1186/s12943-017-0720-x>.
- Crottès D, Jan LY. The multifaceted role of TMEM16A in cancer. *Cell Calcium* 2019;82:102050. doi: <https://doi.org/10.1016/j.ceca.2019.06.004>.
- Duvvuri U, Shiwerski DJ, Xiao D, Bertrand C, Huang X, Edinger RS, et al. TMEM16A induces MAPK and contributes directly to tumorigenesis and cancer progression. *Cancer Res* 2012;72(13):3270–81.
- Liu J, Liu Y, Ren Y, Kang L, Zhang L. Transmembrane protein with unknown function 16A overexpression promotes glioma formation through the nuclear factor-kappaB signaling pathway. *Mol Med Rep* 2014;9:1068–74. doi: <https://doi.org/10.3892/mmr.2014.1888>.
- Liu F, Cao QH, Lu DJ, Luo B, Lu XF, Luo RC, et al. TMEM16A overexpression contributes to tumor invasion and poor prognosis of human gastric cancer through TGF-beta signaling. *Oncotarget* 2015;6:11585–99. doi: <https://doi.org/10.18632/oncotarget.3412>.
- Ayoub C, Wasylyk C, Li Y, Thomas E, Marisa L, Robé A, Roux M, Abecassis J, de Reyniès A, Wasylyk B. ANO1 amplification and expression in HNSCC with a high propensity for future distant metastasis and its functions in HNSCC cell lines. *Br J Cancer* 2010;103(5):715–26.
- Shiwerski DJ, Shao C, Bill A, Kim J, Xiao D, Bertrand CA, Seethala RS, Sano D, Myers JN, Ha P, Grandis J, Gaither LA, Puthenveedu MA, Duvvuri U. To “Grow” or “Go”: TMEM16A expression as a switch between tumor growth and metastasis in SCCN. *Clin Cancer Res* 2014;20(17):4673–88.
- Cao Q, Liu F, Ji K, Liu Ni, He Y, Zhang W, Wang L. MicroRNA-381 inhibits the metastasis of gastric cancer by targeting TMEM16A expression. *J Exp Clin Cancer Res* 2017;36(1). doi: <https://doi.org/10.1186/s13046-017-0499-z>.
- Zeng X, Pan D, Wu H, Chen H, Yuan W, Zhou Ji, Shen Z, Chen S. Transcriptional activation of ANO1 promotes gastric cancer progression. *Biochem Biophys Res Commun* 2019;512(1):131–6.
- Xiao Q, Cui Y. Acidic amino acids in the first intracellular loop contribute to voltage- and calcium- dependent gating of anoctamin1/TMEM16A. *PLoS One* 2014;9. doi: <https://doi.org/10.1371/journal.pone.0099376>.
- Xiao Q, Liu F, Perez-Cornejo P, Cui Y, Arreola J, Hartzell HC. Voltage- and calcium-dependent gating of TMEM16A/Ano1 chloride channels are physically coupled by the first intracellular loop. *Proc Natl Acad Sci* 2011;108(21):8891–6.
- Wei L, Surma M, Shi S, Lambert-Cheatham N, Shi J. Novel Insights into the Roles of Rho Kinase in Cancer. *Arch Immunol Ther Exp (Warsz)* 2016;64(4):259–78.
- Matsui T, Maeda M, Doi Y, Yonemura S, Amano M, Kaibuchi K, et al. Rho-kinase phosphorylates COOH-terminal threonines of ezrin/radixin/moesin (ERM) proteins and regulates their head-to-tail association. *J Cell Biol* 1998;140:647–57. doi: <https://doi.org/10.1083/jcb.140.3.647>.
- Matsuba S, Niwa S, Muraki K, Kanatsuka S, Nakazono Y, Hatano N, Fujii M, Zhan P, Suzuki T, Ohya S. Downregulation of Ca²⁺-activated Cl⁻ channel TMEM16A by the inhibition of histone deacetylase in TMEM16A-expressing cancer cells. *J Pharmacol Exp Ther* 2014;351(3):510–8.
- Liu S. The ROCK signaling and breast cancer metastasis. *Mol Biol Rep* 2011;38(2):1363–6.
- Wang Z. ErbB receptors and cancer. *Methods Mol Biol* 2017;1652:3–35. doi: https://doi.org/10.1007/978-1-4939-7219-7_1.
- Banerjee K, Resat H. Constitutive activation of STAT3 in breast cancer cells: a review: constitutive STAT3 activation in breast cancer. *Int J Cancer* 2016;138(11):2570–8.
- Ivetic A, Ridley AJ. Ezrin/radixin/moesin proteins and Rho GTPase signalling in leukocytes. *Immunology* 2004;112(2):165–76.
- Wu Q, Chen D, Luo Q, Yang Q, Zhao C, Zhang D, et al. Extracellular matrix protein 1 recruits moesin to facilitate invadopodia formation and breast cancer metastasis. *Cancer Lett* 2018;437:44–55.
- Yu L, Zhao L, Wu H, Zhao H, Yu Z, He M, et al. Moesin is an independent prognostic marker for ER-positive breast cancer. *Oncol. Lett.* 2019;17:1921–33. doi: <https://doi.org/10.3892/ol.2018.9799>.
- Perez-Cornejo P, Gokhale A, Duran C, Cui Y, Xiao Q, Hartzell HC, et al. Anoctamin 1 (Tmem16A) Ca²⁺-activated chloride channel stoichiometrically interacts with an ezrin-radixin-moesin network. *Proc Natl Acad Sci* 2012;109(26):10376–81.
- Kulkarni S, Bill A, Godse NR, Khan NI, Kass JI, Steehler K, et al. TMEM16A/ANO1 suppression improves response to antibody-mediated targeted therapy of EGFR and HER2/ERBB2: TMEM16A SUPPRESSION IMPROVES RESPONSE TO ANTI-HER THERAPIES. *Genes Chromosom Cancer* 2017;56(6):460–71.
- Prevarskaya N, Skryma R, Shuba Y. Ion channels in cancer: are cancer hallmarks oncochannelopathies?. *Physiol Rev* 2018;98(2):559–621.
- Jacobsen KS, Zeeberg K, Sauter DRP, Poulsen KA, Hoffmann EK, Schwab A. The role of TMEM16A (ANO1) and TMEM16F (ANO6) in cell migration. *Pflugers Arch - Eur J Physiol* 2013;465(12):1753–62.
- Fife CM, McCarroll JA, Kavallaris M. Movers and shakers: cell cytoskeleton in cancer metastasis: cytoskeleton and cancer metastasis. *Br J Pharmacol* 2014;171(24):5507–23.
- Esteche A, Sanchez-Martin L, Puig-Kroger A, Bartolome RA, Teixido J, Samaniego R, et al. Moesin orchestrates cortical polarity of melanoma tumour cells to initiate 3D invasion. *J Cell Sci* 2009;122(19):3492–501.
- Clucas J, Valderrama F. ERM proteins in cancer progression. *J Cell Sci* 2015;128(6):1253.